AUTOPHAGY
2022, VOL. 18, NO. 7, 1534–1550
https://doi.org/10.1080/15548627.2021.1990669

Taylor & Francis
Taylor & Francis Group

RESEARCH PAPER

Human platelets display dysregulated sepsis-associated autophagy, induced by altered LC3 protein-protein interaction of the Vici-protein EPG5

Hansjörg Schwertz[a,b,c,k], Jesse W. Rowley[a,d], Irina Portier[a], Elizabeth A. Middleton[a,d], Neal D. Tolley[a], Robert A. Campbell[a,f], Alicia S. Eustes[a,i], Karin Chen[a,e,j], and Matthew T. Rondina[a,f,g,h]

[a]Molecular Medicine Program, University of Utah, Salt Lake City, UT, USA; [b]Work Wellness Clinic, University of Utah, Salt Lake City, UT, USA; [c]Division of Occupational Medicine, University of Utah, Salt Lake City, UT, USA; [d]Division of Pulmonary Medicine, University of Utah, Salt Lake City, UT, USA; [e]Department of Pediatrics, University of Utah, Salt Lake City, UT, USA; [f]Departments of Internal Medicine, University of Utah, Salt Lake City, UT, USA; [g]Department of Pathology, University of Utah, Salt Lake City, UT, USA; [h]Department of Internal Medicine, George E. Wahlen Salt Lake City VAMC, Salt Lake City, UT 84112, USA; [i]Department of Internal Medicine, University of Iowa in Iowa City, IA, USA; [j]Department of Pediatrics, University of Washington School of Medicine, and Seattle Children's Hospital, Seattle, WA, USA; [k]Occupational Medicine, Billings Clinic Bozeman, Bozeman, MT, USA

ABSTRACT

Platelets mediate central aspects of host responses during sepsis, an acute profoundly systemic inflammatory response due to infection. Macroautophagy/autophagy, which mediates critical aspects of cellular responses during inflammatory conditions, is known to be a functional cellular process in anucleate platelets, and is essential for normal platelet functions. Nevertheless, how sepsis may alter autophagy in platelets has never been established. Using platelets isolated from septic patients and matched healthy controls, we show that during clinical sepsis, the number of autophagosomes is increased in platelets, most likely due to an accumulation of autophagosomes, some containing mitochondria and indicative of mitophagy. Therefore, autophagy induction or early-stage autophagosome formation (as compared to decreased later-stage autophagosome maturation or autophagosome-late endosome/lysosome fusion) is normal or increased. This was consistent with decreased fusion of autophagosomes with lysosomes in platelets. EPG5 (ectopic P-granules autophagy protein 5 homolog), a protein essential for normal autophagy, expression did increase, while protein-protein interactions between EPG5 and MAP1LC3/LC3 (which orchestrate the fusion of autophagosomes and lysosomes) were significantly reduced in platelets during sepsis. Furthermore, data from a megakaryocyte model demonstrate the importance of TLR4 (toll like receptor 4), LPS-dependent signaling for regulating this mechanism. Similar phenotypes were also observed in platelets isolated from a patient with Vici syndrome: an inherited condition caused by a naturally occurring, loss-of-function mutation in EPG5. Together, we provide evidence that autophagic functions are aberrant in platelets during sepsis, due in part to reduced EPG5-LC3 interactions, regulated by TLR4 engagement, and the resultant accumulation of autophagosomes.

Abbreviations: ACTB: beta actin; CLP: cecal ligation and puncture; Co-IP: co-immunoprecipitation; DAP: death associated protein; DMSO: dimethyl sulfoxide; EPG5: ectopic P-granules autophagy protein 5 homolog; ECL: enhanced chemiluminescence; HBSS: Hanks' balanced salt solution; HRP: horseradish peroxidase; ICU: intensive care unit; LPS: lipopolysaccharide; LAMP1: lysosomal associated membrane protein 1; MAP1LC3/LC3: microtubule associated protein 1 light chain 3; MTOR: mechanistic target of rapamycin kinase; MKs: megakaryocytes; PFA: paraformaldehyde; PBS: phosphate-buffered saline; PLA: proximity ligation assay; pRT-PCR: quantitative real-time polymerase chain reaction; RT: room temperature; SQSTM1/p62: sequestosome 1; SDS-PAGE: sodium dodecyl sulfate-polyacrylamide gel electrophoresis; TLR4: toll like receptor 4; TEM: transmission electron microscopy; WGA: wheat germ agglutinin.

ARTICLE HISTORY
Received 14 December 2020
Revised 30 September 2021
Accepted 4 October 2021

KEYWORDS
Autophagic flux; co-immunoprecipitation; epg5; lipopolysaccharide; megakaryocytes; platelets; protein interactions; sepsis; toll like receptor 4; vici syndrome

Introduction

Sepsis is a common, and often morbid, syndrome characterized by systemic inflammation and dysregulated immune responses triggered by invading pathogens or toxins produced by pathogens, as well as injurious agonists generated by the host. In cases of severe sepsis, intravascular hypotension and organ dysfunction are common [1]. Adverse clinical outcomes during sepsis are also driven by endothelial and micro- and macro-vascular dysfunction, cellular metabolic reprogramming, and thrombosis [1]. During the course of sepsis, pro- and anti-inflammatory mediators are generated [2] and effector cells are activated [3,4]. Despite sustained efforts, sepsis continues to cause significant mortality and morbidity worldwide. Even after surviving sepsis, patients are at increased long-term risk of myocardial infarction and venous thromboembolic disease [5–7]. Recent therapeutic interventions have largely been unsuccessful in

CONTACT Hansjörg Schwertz hansjorg.schwertz@u2m2.utah.edu The University of Utah, Work Wellness Clinic
Supplemental data for this article can be accessed here.

improving outcomes from sepsis and there is a critical need to better understand how sepsis alters cellular functions, to guide the rational development of new treatments for sepsis.

In eukaryotic cells, autophagy is a process allowing the breakdown of intracellular cargo larger than single proteins. Autophagy is also a primary mechanism for replenishing the pool of biosynthetic precursors and energy sources, by recycling cytosolic contents during starvation [8]. Autophagy can be a nonselective (i.e. bulk) or a selective process, and allows for the recycling of harmful or unneeded cellular material, including damaged mitochondria, protein aggregates, excess ribosomes, lipid droplets, or intracellular pathogens [9,10]. To initiate autophagy, membrane remodeling, crescent-shaped phagophore formation, and subsequent building of the double-membrane autophagosome is required (reviewed in [11]). Autophagosomes fuse with the lysosomes and vacuoles, allowing for the degradation of sequestrated materials and organelles [12].

A number of proteins critically mediate distinct phases of the multi-step autophagy process and autophagosome formation [13]. One of these is EPG5 (ectopic P-granules autophagy protein 5 homolog). In 2016, Wang and colleagues discovered that EPG5 is recruited to late endosomes and lysosomes by RAB7 [14]. Late endosomes and lysosomes are subsequently tethered to autophagosomes by EPG5-LC3 interactions, which then lead to the maturation of autolysosomes [14]. Loss-of-function mutations in, or the deficiency of, *EPG5* results in the formation of non-degradative vesicles. This phenotype is observed in Vici syndrome [OMIM242840] [15,16]. Vici syndrome is a rare (~78 patients are known in the literature [17]), severe (multisystem dysfunction with median survival time of 24 months), recessively inherited congenital disorder due to loss-of-function mutations in *EPG5* [15]. EPG5 is a key regulator of autophagosome maturation. The impairment or inhibition of autophagosome fusion with endosomes may result in the accumulation of non-degradative autophagosomes or autolysosomes [18].

Autophagy is an integral part of host responses to sepsis [19]. For example, the formation, maturation, and degradation of autophagosome contents counteracts microbial invasion by aiding in the active elimination of intracellular bacteria and viruses, supports antigen presentation, and removes damaged protein complexes or organelles to maintain homeostasis in the infected organism [20]. Autophagy may serve a protective role in sepsis by preserving mitochondrial integrity and reducing apoptotic cell death [20,21]. In experimental animal models of sepsis, tissue autophagic activity was increased during the initial phases of sepsis [21–23]. However, studies focusing on the kinetics of autophagy in sepsis in liver tissue demonstrated a decline in autophagic activity and late-stage inhibition several hours into the induction of sepsis [21,23,24]. Autophagy has also been a therapeutic target in sepsis, in efforts to restore dysregulated immune reactions (reviewed in [25]). Overexpression of LC3 in a cecal ligation and puncture (CLP)-induced sepsis mouse model did increase the autophagosome clearance and the overall survival [26]. In addition, restoration of autophagic flux using rapamycin in a CLP mouse model did result in cardiac protection and preserved cardiac performance [27].

Platelet aggregation and the formation of heterotypic platelet-leukocyte aggregates in septic patients is associated with increased morbidity and mortality [28–30]. However, the direct impact of platelets in the pathobiology of sepsis remains incompletely understood. Due to their high number in the circulation, platelets are often one of the first blood cells to encounter circulating pathogens. Platelets are increasingly appreciated for their roles in host immune responses, including surveilling for, recognizing, and containing invading bacterial pathogens [31–35]. Recent studies from our laboratory revealed that megakaryocytes, the platelet progenitor cell, possesses endogenous anti-viral immune functions through the signal-dependent synthesis and release of immunomodulatory cytokines [36,37].

In 2014, Feng and colleagues demonstrated that the autophagic machinery is constitutively expressed in human platelets, and that autophagy is required for fundamental platelet functions [38]. In subsequent studies, it was demonstrated that reduced or abolished autophagy altered megakaryopoiesis and platelet formation [39,40]. Furthermore, using a murine model where ATG7 (autophagy related 7), an autophagy

Table 1. Clinical features in patient with Vici-syndrome.

Sex	male
Birthweight	3,415 g
Status	died at 7 months
Developmental Delay	+
Hypotonia	+
Hypopigmentation	+
Cardiac Involvement	+ (aortic coarctation, fenestrated septum, right ventricular hypertrophy)
Seizures	-
Central Nervous System Anomalies	+ (absent corpus callosum, polymicrogyria of the bilateral opercular and insular cortices, enlargement of subarachnoid spaces, persistence of fetal venous structures in the lateral cerebral fissure)
Immunologic Findings	+ (mildly low IgG and IgM, metapneumovirus-associated respiratory distress, normal lymphocyte proliferation)
Chronic medical Needs	oxygen supplementation since birth
Facial Findings	+ (shortened nose with upturned nares, edema)
Muscular-Skeletal Findings	+ (epicanthal folds, transverse palmar crease, tapered fingers, elongated 4th toe with clinodactyly)
Laboratory Findings	Mild thrombocytopenia (90,000–120,000)
Chromosomal Findings	mosaicism XXY (65%), XY (35%)
Genomic Findings	XXY (80%), Xp22.33q28(168,546–155,233,731)x1-2,18q12.1q21.2(29,156,720–48,384,599), mosaic Klinefelter syndrome
Gene Sequencing	*EPG5*, homozygous c.2066delT (p.L689*)

The included patient does demonstrate several diagnostic criteria for Vici-syndrome (i.e., callosal agenesis, cardiac involvement, hypopigmentation). While the additional Klinefelter syndrome mosaic is present, the severe clinical findings are not linked to typical clinical features found in XXY patients.

protein integral for proper functions, was specifically deleted in platelets, Ouseph and colleagues identified the importance of platelet autophagy for thrombosis and hemostasis [41] (also reviewed in [42]).

Whether platelet autophagy is altered during sepsis has not been studied in detail. Accordingly, we sought to determine the dynamics of autophagy in human platelets under septic conditions, and to examine molecular mechanisms involved in the regulation of this intricate pathway.

Results

Human platelets isolated from Vici syndrome-patient demonstrate increased LC3 protein levels and accumulate SQSTM1/p62

Platelets isolated from a patient with Vici syndrome demonstrated increased LC3 and SQSTM1/p62 (sequestosome 1) protein levels, and accumulation of LC3-positive particles. The clinical characteristics of the patient with Vici syndrome, with confirmed homozygous mutation in *EPG5* c.2066delT (p. L689*) are shown in Table 1. While the patient also had a mosaic Klinefelter syndrome, the clinical features typically found in patients with Vici syndrome were present. Interestingly, this patient with Vici syndrome had a mild thrombocytopenia (platelet count ranging between 90–120 K/μL, Table 1), without clinically relevant bleeding.

Although Vici syndrome has been characterized in more detail in recent years [14,15,43], how this syndrome affects platelets remains unknown. We assessed platelet morphology, granule content, and autophagy-related protein expression with a small amount of blood limited by the subject weight. Platelets from this patient with Vici syndrome exhibited normal morphology and granule content (WGA staining for cell membrane and granules, 777.4 vs. 693.0, fluorescent intensity for WGA per cell, healthy vs. Vici syndrome, per cell-to cell analysis), comparable to platelets isolated from a gender-matched healthy donor (Figure 1A, second lane from left).

Vici syndrome is caused by mutations in the gene *EPG5* (OMIM # 615,068), which leads to impairments in the fusion of autophagosomes and lysosomes. To determine if autophagy in platelets is disrupted in Vici syndrome, we assessed expression of MAP1LC3/LC3 (microtubule associated protein 1 light chain 3) protein levels via immunofluorescence microscopy, an accepted method of determining autophagy activity [44]. Compared to platelets from a matched healthy control subject, LC3 protein levels in Vici syndrome were approximately 1.5–1.9 higher as analyzed by immunofluorescence microscopy and overall mean fluorescent intensity, percent LC3-positive cells, or the number of LC3-positive particles per cell (Figures 1A and 1B).

We next assessed changes in LC3-I and LC3-II by immunoblot, as well as LC3 conversion to determine if LC3-II accumulated in platelets when autophagy was activated with rapamycin. Rapamycin does bind to the MTOR (mechanistic target of rapamycin kinase) FRB domain, limiting its interaction with RPTOR (regulatory associated protein of MTOR complex 1), and thus inducing autophagy [45]. As shown in Figure 1C, and consistent with our observations by immunofluorescence microscopy (Figures 1A and 1B), LC3-I and -II protein were increased in platelets from the patient with Vici syndrome, both at baseline and under rapamycin-stimulated conditions. LC3-II, but not LC3-I, increased further in platelets from the patient with Vici syndrome upon stimulation with rapamycin. In addition, conversion of LC3 (as determined by the LC3 II:I ratio, data not shown) was also increased in platelets from the patient with Vici syndrome.

To further evaluate autophagy function, we measured levels of the autophagosome cargo protein SQSTM1 at baseline and with rapamycin stimulation (a way to examine SQSTM1 accumulation) in platelets from the patient with Vici syndrome. Baseline levels of SQSTM1 were increased in platelets from the patient with Vici syndrome, and SQSTM1 protein decreased ~40% upon stimulation with rapamycin (Figure 1D). Finally, we examined EPG5 levels in patient platelets, the protein affected in our patient with Vici syndrome [46] (Table 1). EPG5 protein expression in platelets isolated from the patient with Vici syndrome were almost undetectable, both at baseline and in response to stimulation with rapamycin (Figure 1E). Taken together, these findings indicate that the mutation of EPG5 in Vici syndrome results in decreased clearance of autolysosomes, and accumulation of autophagosome cargo in human platelets.

Autophagic vacuoles accumulate in septic platelets

Vici syndrome is characterized by recurrent respiratory infections, and accumulation of autophagosomes in various tissues [15]. Our findings of altered autophagic function and increased autophagosomes in platelets from a patient with Vici syndrome resembled morphologic findings observed in microscopic and ultrastructural analysis of human platelets isolated from septic patients as presented in this study. These similarities between the inherited immune diseases caused by genetic mutations and a systemic inflammatory insult characterized by immune dysregulation led us to hypothesize that alterations of autophagy in platelets in sepsis may be induced by analogous molecular mechanisms (i.e., alteration of EPG5 function, not mutation of *EPG5*) as are present in Vici syndrome patients.

Since transmission electron microscopy (TEM) reveals the morphology of autophagic structures at a resolution in the nm range, we examined platelets from septic patients and healthy control platelets on an ultrastructural level. Autophagosomes, also referred to as initial autophagic vacuoles, which typically display a double membrane [44], were present in platelets isolated from septic patients, but significantly reduced in platelets from healthy control donors (Figure 2A and B). In addition, platelets from septic patients had autophagosomes containing cell organelles (i.e., mitochondria, Figure 2A, yellow arrows), indicative of mitophagy. Late, degenerative autophagic vacuoles/autolysosomes, which are characterized by only one limiting membrane and typically with degraded content, were less frequently detected than autophagosomes.

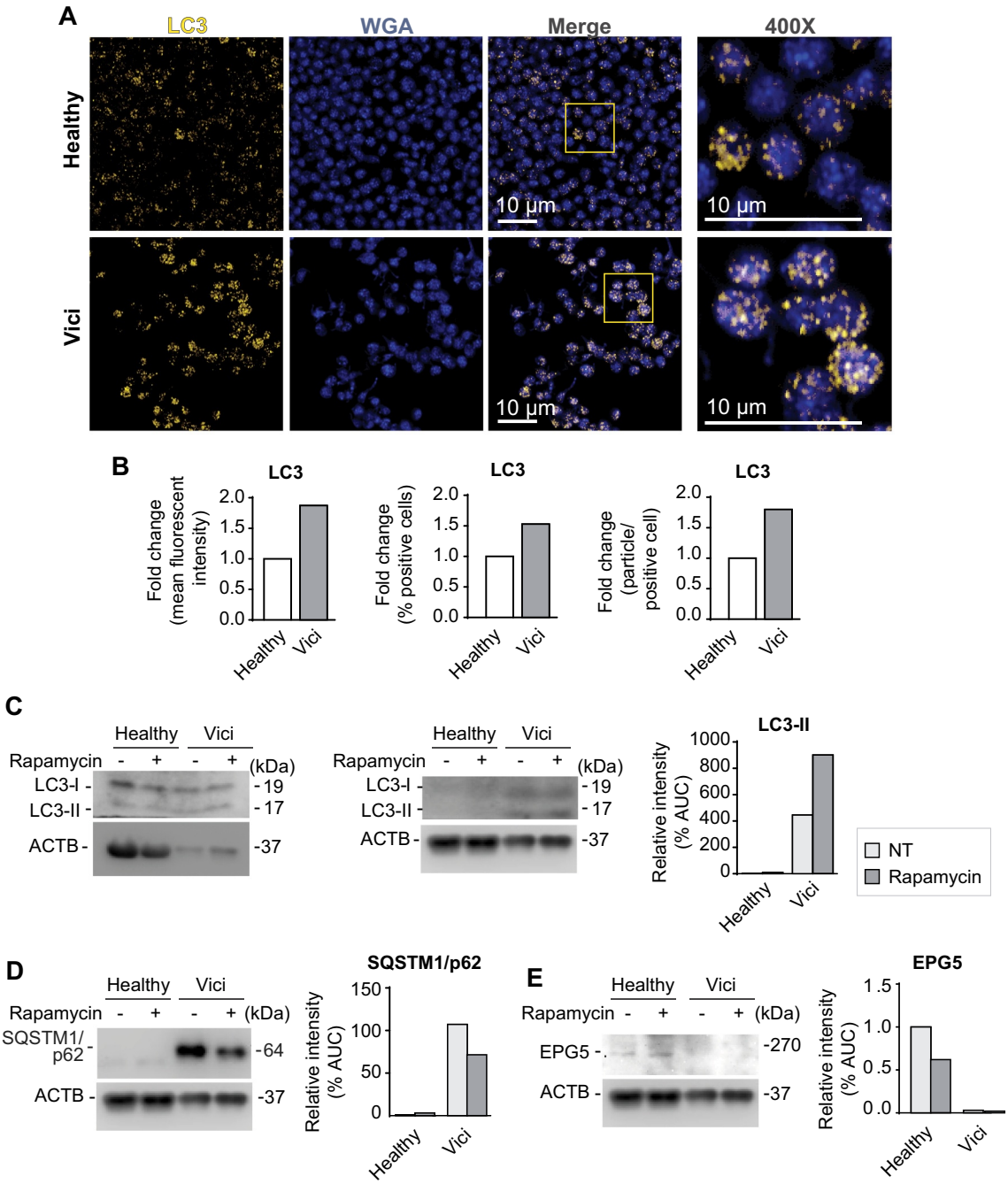

Figure 1. Human platelets isolated from Vici syndrome-patient demonstrate increased LC3 protein levels and accumulate SQSTM1/p62. (A) Freshly isolated platelets from a healthy subject or pediatric patient with Vici syndrome were fixed in suspension immediately after isolation. Representative images are shown. Immunofluorescence staining with an anti-LC3 (yellow) antibody demonstrates expression of increased levels of LC3 in platelets from patient with Vici syndrome when compared to healthy platelets (scale bars: 10 μm). Cells were co-stained using WGA (which binds to glycoproteins of the cell and granule membrane, blue). The yellow box in the merge image demonstrates the origins of the 400x images. (B) Micrographs were analyzed using CellProfiler. The bar graphs display the fold change of mean fluorescent intensity (left, healthy in white and patient with Vici syndrome in gray), fold change of positively stained cells (middle), and fold change of stained particles/positive stained cell (right). (C) Immunoblot analysis of platelet lysates from healthy and Vici patient platelets (± rapamycin to induce autophagy) using an anti-LC3 antibody. Corresponding ACTB/actin as a loading control is depicted (bottom). Molecular masses of the respective proteins are indicated. Left blot with unequal ACTB loading demonstrates that LC3 is present in healthy platelets. The quantitative analysis of LC3-II:ACTB ratio, is shown. (D) Immunoblot analysis of platelet lysates from healthy and Vici-patient platelets (± rapamycin to induce autophagy) using an anti-SQSTM1/p62. Corresponding ACTB as a loading control is depicted (bottom). The quantitative analysis of SQSTM1/p62:ACTB ratio is shown. (E) Immunoblot analysis of platelet lysates from healthy and Vici-patient platelets (± rapamycin to induce autophagy) using an anti-EPG5 antibody. Corresponding ACTB as a loading control is depicted (bottom). The quantitative analysis of EPG5:ACTB ratio is shown. For bar graphs in C, D, and E, non-treated (NT, light gray), and rapamycin (dark gray).

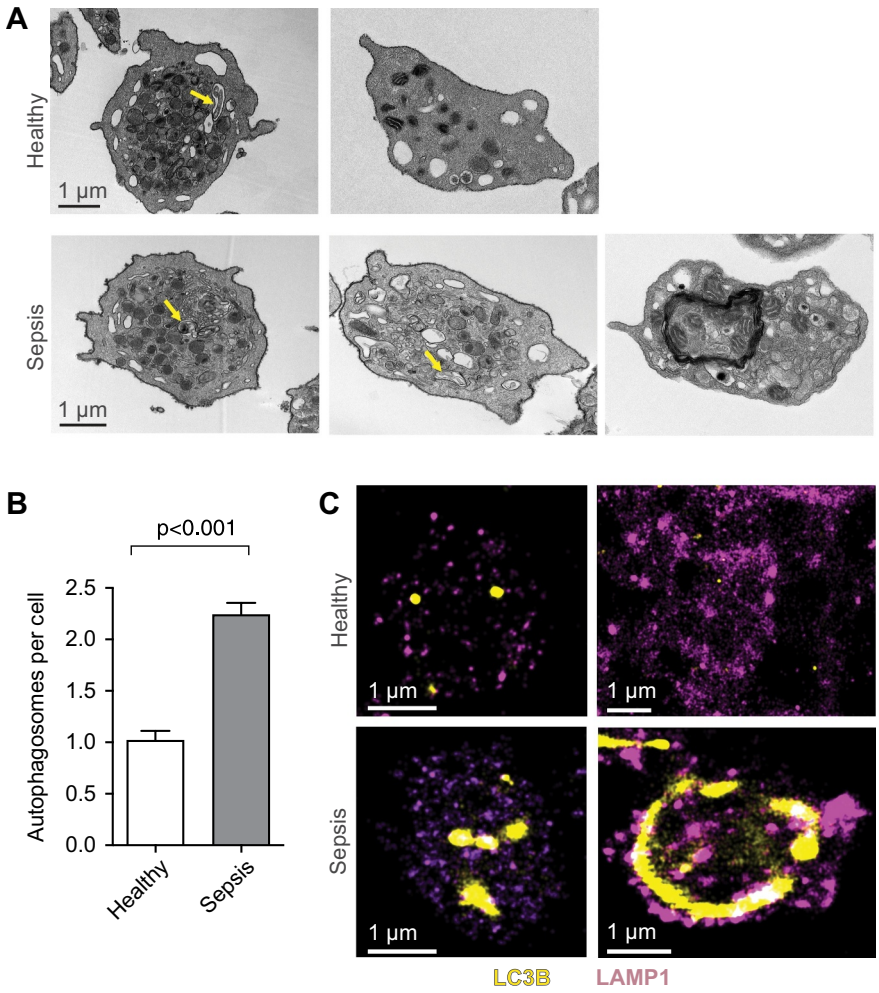

Figure 2. Platelets isolated from septic patient demonstrate increased autophagosomal activity when compared to platelets isolated from healthy individuals. (A) Transmission electron microscopic analysis of healthy platelets (top row) and platelets isolated from septic patients (bottom row, scale bars: 1 µm). Yellow arrows indicate autophagosomes of various content. This figure is representative of n = 5 independent experiments. (B) Bar graph showing the quantitative analysis of autophagosomes being present in healthy versus septic human platelets. The figure represents the analysis of >100 cells per group from n = 5 subjects per group. (C) Images demonstrate healthy platelets (top row) and platelets isolated from septic patients (bottom row) immunostained with an anti-LC3 (yellow), and an anti-LAMP1 (magenta) antibody. Cells were subsequently analyzed using super resolution microscopy. Scale bars: 1 µm. White color expression demonstrates potential colocalization. This figure is representative of n = 4 independent experiments.

Table 2. Demographic data for the cohort of septic patients.

Characteristic	Septic Patients (n = 16)
Age, years	median 68, range 30–86
Sex, male n (%)	10 (62.25)
Septic Shock, n (%)	6 (37.5)
Mechanical Ventilation, n (%)	4 (25.0)
28-day Mortality, n (%)	2 (12.5)
Platelet Count at ICU Admission, (k/µl)	median 202, range 50–304
Infection Source,	
Respiratory n (%)	8 (50.0)
Urinary tract n (%)	6 (37.5)
Skin/soft tissue n (%)	2 (12.5)
Unknown cause n (%)	1(6.25)
Vasopressor Use, n (%)	9 (56.25)

Table 3. Demographic data for the cohort of healthy controls.

Characteristics	Healthy Controls (n = 12)
Age, years	median 43, range 25–50
Sex, male n (%)	5 (41.7)

Demographic data shown from septic patients and healthy controls were collected at the time of study enrollment, which was within 48 (±24) h of ICU admission for sepsis. Some patients had multiple infectious sources. Data shown are the median, range, or n (%).

We next examined the localization of LC3 and LAMP1 (lysosomal associated membrane protein 1; a lysosomal marker) by immunofluorescent staining in platelets from septic patients (Table 2) and, for comparison, gender-matched healthy control donors (Table 3). Platelet aggregate formation, and LC3 expression increased significantly in septic patients, when compared to healthy platelets (Figure S1A and B). LAMP1 expression was also moderately increased in septic patient samples, and intracellular location was preserved.

Next, we utilized super-resolution microscopy geared toward the detection of the localization of proteins, to generate image resolutions below the technical optical limit (i.e., 20 nm lateral resolution) in combination with immunofluorescence. We confirmed in platelets from a healthy donor our ability to detect the formation of LC3 and autophagosomes upon stimulation with rapamycin, which increases autophagic activity, and with bafilomycin A_1, which inhibits the fusion of

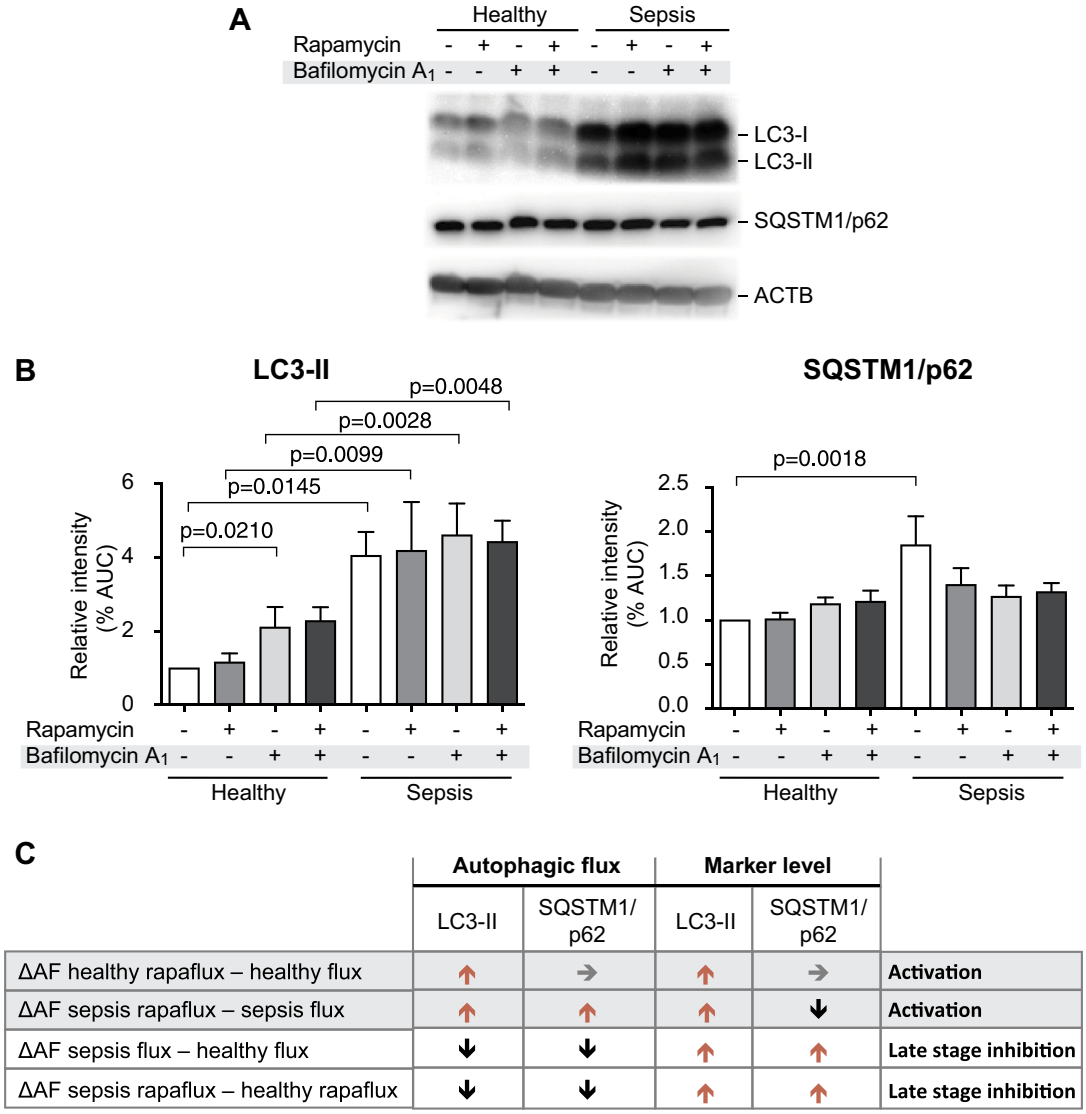

C

	Autophagic flux		Marker level		
	LC3-II	SQSTM1/p62	LC3-II	SQSTM1/p62	
ΔAF healthy rapaflux – healthy flux	↑	→	↑	→	**Activation**
ΔAF sepsis rapaflux – sepsis flux	↑	↑	↑	↓	**Activation**
ΔAF sepsis flux – healthy flux	↓	↓	↑	↑	**Late stage inhibition**
ΔAF sepsis rapaflux – healthy rapaflux	↓	↓	↑	↑	**Late stage inhibition**

Figure 3. Platelets isolated from septic patients demonstrate late-stage inhibition of autophagy when compared to healthy platelets. (A) Platelets from healthy individuals and septic patients were isolated and treated with rapamycin and/or bafilomycin A_1. SQSTM1/p62 accumulation, LC3-I conversion and LC3-II turnover were detected by western blot. Positions of LC3-I and -II are marked. Corresponding ACTB is shown at the bottom and was used for normalization (B). The quantitative analysis of the flux experiments is shown. The graphs are representative of n = 7 independent experiments. AUC, area under curve. (C) SQSTM1/p62 turnover was used as a measure of autophagic flux (AF). Autophagic flux was calculated as referenced in material and methods. The ΔAF was converted from numbers to arrows to directional changes. Stages of autophagy were defined by pattern of ΔAF and corresponding LC3 and SQSTM/p62 levels.

autophagosomes with lysosomes and triggers LC3 accumulation (Figure S2).

Next, we investigated the localization of immuno-detected autophagosomes in unstimulated platelets from septic patients, compared to healthy donors. Consistent with our findings by TEM and ICC (Figure 2A B and Figure S2), we observed an increased intracellular localization for LC3, suggesting an increased number of autophagosomes in platelets from septic patients (Figure 2C).

Sepsis was associated with late-stage inhibition of autophagic flux in platelets

Autophagic flux, the process in which autophagosomes transition to autolysosomes, delineates autophagic degradation [44]. Autophagic flux can be inferred on the basis of LC3-II turnover measured by western blotting [47]. In addition, SQSTM1 becomes incorporated into the formed autophagosome and is degraded in the autolysosomes. Thus, measuring LC3-II turnover and changes in SQSTM1 can be used to quantify changes in cellular autophagic flux [47]. Based on our morphologic (e.g., TEM, Figure 2A) and super-resolution immuno-detection studies (Figure 2C), we hypothesized that autophagic flux would be altered in platelets from septic patients.

We first investigated LC3-I, LC3-II, and SQSTM1 protein levels in platelets from septic patients, examining both baseline, unstimulated levels and changes in response to platelets stimulated with rapamycin or bafilomycin A_1 in order to determine if autophagic flux was altered in sepsis. Levels of all three of these proteins were significantly higher in unstimulated platelets from septic patients (Figures 3A and 3B). While autophagic flux could be further induced in rapamycin-stimulated platelets from septic

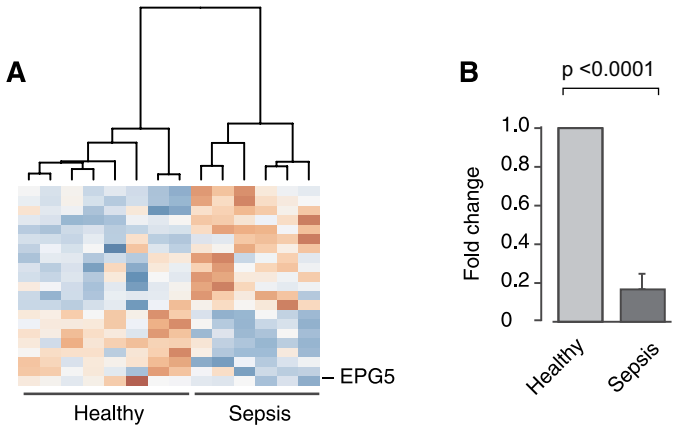

Figure 4. Transcripts coding for key factors of autophagy are differentially expressed in platelets isolated from septic patient when compared to platelets from healthy individuals. Platelets were isolated from healthy individuals or septic patients within 48 h of ICU admission. Total RNA was isolated and next generation RNA-sequencing (RNA-seq) was performed (n = 6–8 per group, respectively). (A) Heat map of upregulated (log_2 fold-change > 0, red) and downregulated (log_2 fold-change < 0, blue) transcripts in platelets from healthy individuals and septic patients. Black brackets indicate hierarchical grouping. (B) *EPG5* expression was verified using qRT-PCR in independent septic patients and healthy controls. The bar graph shows the fold change by ΔΔCT-method (n = 7 subjects per group).

patients, sepsis was associated with late-stage inhibition of autophagy in platelets (Figure 3C) when compared to healthy platelets. Based on these results and our microscopy studies (Figure 2), these findings suggest that reduced autophagic activity and late-stage inhibition of the autophagic flux in platelets from septic patients may be due to impaired fusion of lysosomal vesicles with autophagosomes.

Transcripts coding for key autophagy proteins are differentially expressed in platelets from septic patients

Although anucleate, emerging data demonstrates that the human platelet transcriptome is not static. Rather, the platelet transcriptome is dynamic and often markedly altered during systemic inflammatory diseases [36,37,48,49]. To determine whether transcripts coding for autophagy proteins were altered in platelets during sepsis, we used RNA-seq on highly purified platelets from septic patients and matched healthy donors. This was performed as a sub-analysis of a dataset previously published by our group [50]. Table S1 demonstrates that limited transcripts encoding for proteins involved in autophagy were significantly altered in sepsis. Figure 4A shows the up- and downregulated transcripts in a heat map, including the expression of *EPG5*.

Among the differentially expressed transcripts, *EGP5* was significantly reduced (log2 fold-change = −0.7598; p (adjusted) = 0.0491) in platelets from septic patients. To validate changes in *EPG5* expression, we performed qRT-PCR on platelets from an independent set of septic patients and matched healthy donors. Consistent with data generated by RNA-seq, *EPG5* expression was significantly downregulated (~80%, p < 0.0001) in platelets during sepsis (Figure 4B).

EPG5 protein expression levels are increased in platelets due to inflammatory conditions

Having detected significantly reduced *EPG5* transcript levels in platelets from septic patients, we hypothesized that EPG5 protein expression would similarly be altered during sepsis. In contrast to the reduced RNA expression of *EPG5*, western blot analysis demonstrates significantly increased EPG5 protein expression in platelets from septic patients (Figure 5A). To further test the above hypothesis, we used immunofluorescence-staining (ICC) to examine EPG5 protein subcellular localization in platelets from septic patients and matched healthy control donors. EPG5 staining was localized in a granular pattern in platelets from septic patients (Figure 5B). Additionally, using automated image analysis, we detected a significantly increased number of EPG5-positive cells (Figure 5C), which was accompanied by corresponding increase in EPG5 signal per positive cells (data not shown). Contrasting RNA-protein expression patterns were also previously observed in platelets for MMPs (matrix metallopeptidases) and TIMP (TIMP metallopeptidase inhibitor) [51]. Discrepancies in mRNA and protein expression may be explained by differential loading of RNA and protein in platelets by their precursor cell megakaryocytes, RNA stability, and/or altered dynamics of the regulation of transcription and translational control mechanisms.

EPG5-LC3 interactions are reduced in human platelets during sepsis

Previous studies demonstrate that EPG5 facilitates the fusion of autophagosomes and late endosomes/lysosomes during late stages of autophagy by coordinating RAB7 and directly tethering LC3 [14]. Our results demonstrate decreased autophagic flux and late-stage inhibition, but increased protein expression for LC3 and EPG5. Therefore, we next examined whether interactions between EPG5 and LC3 were altered under septic conditions. The functional consequence of decreased LC3-EPG5 interaction would be reduced autophagosome and lysosome fusion, resulting in diminished autophagic flux, late-stage inhibition, and accumulation of autophagosomes, as we observed in platelets from septic patients. Using specific antibody to LC3 for immunoprecipitation and measuring both LC3 and co-immunoprecipitated EPG5 we found that while LC3 readily interacted with EPG5 in platelets from healthy donors, LC3-EPG5 protein-protein interactions were markedly reduced in platelets isolated from septic donors compared to healthy donors (Figure 5D), an observation we could reproduce using proximity ligation technique (Figure S3A and B). Input controls were similar between septic patients and healthy controls (triangle – healthy, circle – septic; Figure 5D, insert). Interesting, LC3-I and LC3-II accumulation in platelets detected by co-immunoprecipitation from septic patients was higher than in matched healthy donors under unstimulated conditions (Figure 5D). Immunoprecipitated LC3 levels did not significantly change in rapamycin or bafilomycin A_1 stimulated platelets from septic patients, compared to unstimulated conditions.

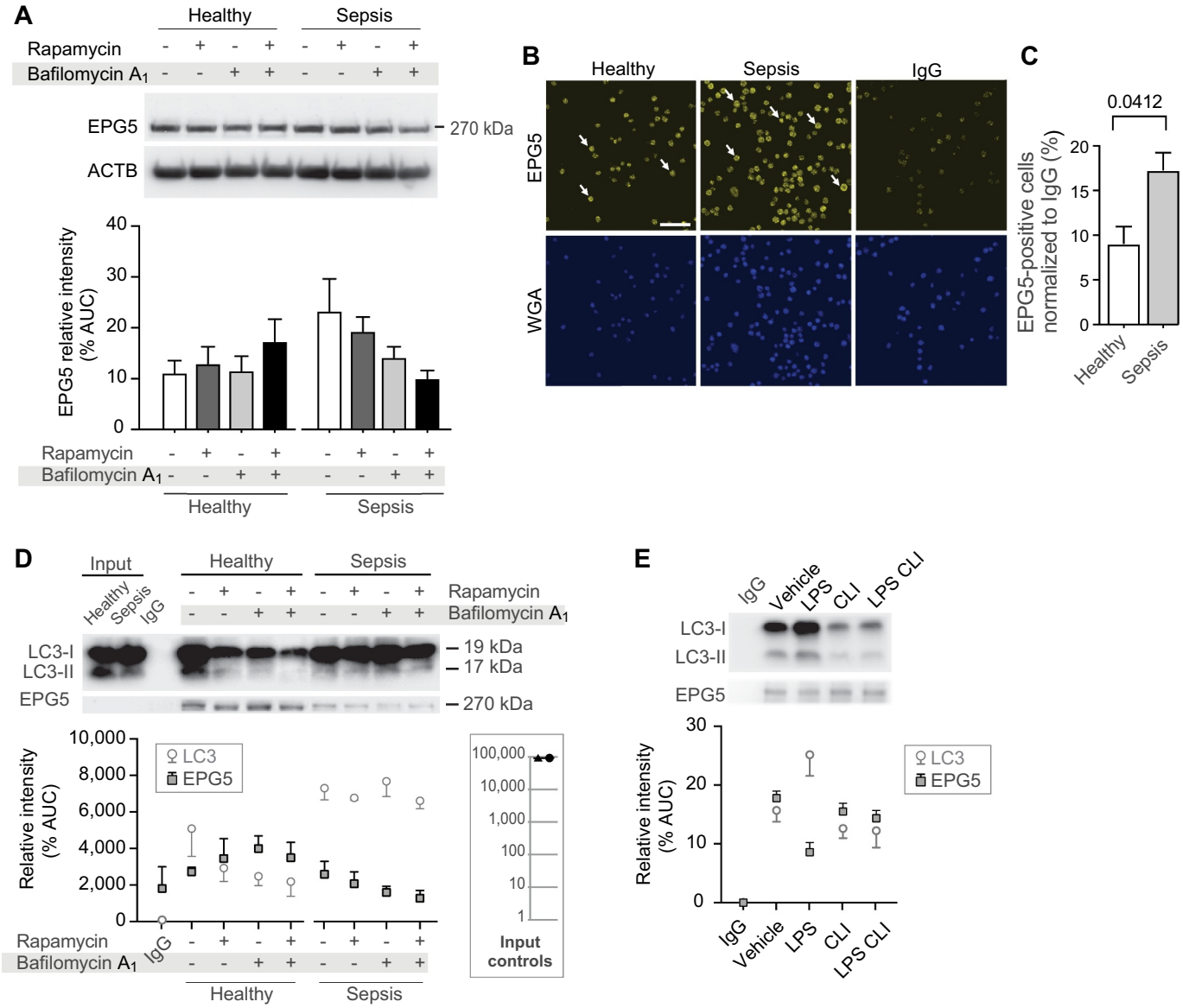

Figure 5. EPG5 protein expression is increased in septic platelets, while EPG5-LC3 interaction decreases during sepsis. (A) Platelets from healthy individuals and septic patients were isolated and treated with rapamycin and/or bafilomycin A_1. EPG5 expression levels were detected by western blot. Position of EPG5 is marked. Corresponding ACTB is shown at the bottom and was used for normalization of data presented in bar graph below. This figure is representative of n = 6 independent experiments. (B) Platelets were fixed in suspension immediately after isolation. Immunofluorescence staining with an anti-EPG5 (yellow) antibody demonstrates robust expression of EPG5 protein in platelets from septic patients and healthy platelets (scale bars: 10 μm). Cells were co-stained using WGA (blue). White arrows highlight platelet cell bodies for orientation. This figure is representative of n = 3 independent experiments. (C) Micrographs were analyzed using CellProfiler. The bar graph displays the percent of positively stained cells for EPG5, normalized to IgG. (D) Endogenous LC3 precipitates endogenous EPG5 in a co-IP assay. Input samples as controls are indicated in inserted box. The open circles demonstrate the densitometric analysis of the co-IP experiment for LC3, the overlaid closed squares show the densitometric analysis of co-IP'd EPG5 for each experimental condition. This figure is representative of n = 7 independent experiments. (E) Endogenous LC3 precipitates endogenous EPG5 in a co-IP assay using MKs cultured under simulated septic conditions (LPS treatment) and treated with specific TLR4 inhibitor, CLI-095. This immunoblot is representative of n = 4 independent experiments. In the graph below the immunoblot, the open circles demonstrate the densitometric analysis of the co-IP experiment for LC3, while the overlaid closed squares show the densitometric analysis of co-IP'd EPG5.

To further establish a molecular signaling pathway potentially regulating the direct EPG5-LC3 interactions during late-stage inhibition of autophagy in platelets during sepsis we utilized an established $CD34^+$-derived human megakaryocyte (MK) cell culture model [52–54]. MKs are platelet precursor cells, contain many of the same proteins and pathways as platelets, and are often used as a relevant model system to study platelet responses [50,55]. The exposure of human MKs to an agonist commonly generated during sepsis (lipopolysaccharide, LPS) resulted in decreased EPG5-LC3 protein-protein interaction patterns (Figure 5E). This experimental finding in human MKs was consistent with our clinical observations in platelets from septic patients (Figure 5D). The diminished EPG5-LC3 protein-protein engagement was reversed by a small molecule inhibitor, CLI-095 (Figure 5E), that suppresses cellular responses triggered by the LPS-TLR4 signaling cascade through blocking downstream effects mediated by the intracellular, cytoplasmic tail domain of the TLR4 [56]. Consistent with these data, in human MKs, LPS increased TLR4 dependent phosphorylation of MAPK1

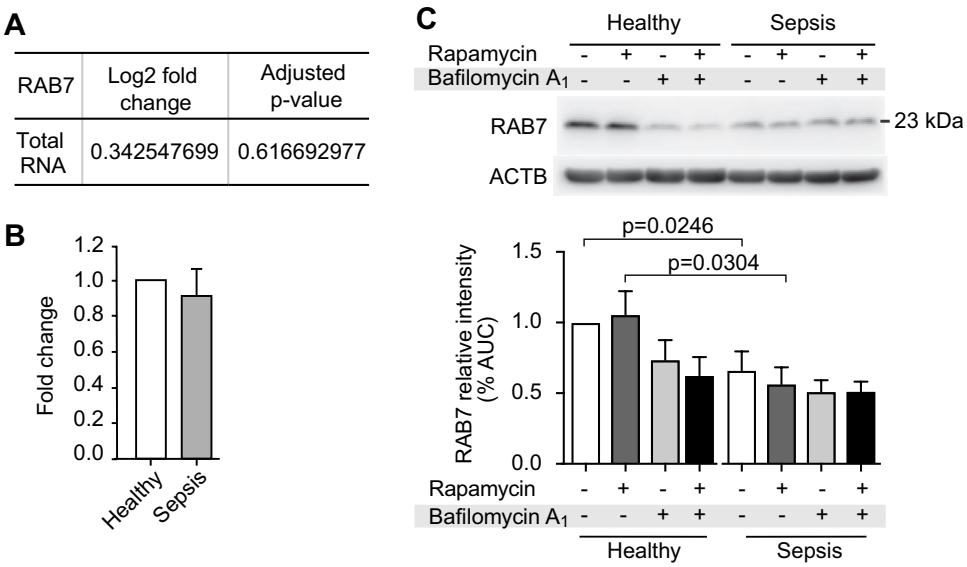

Figure 6. RAB7 RNA and protein expression levels are dynamic during sepsis. (A) Changes in *RAB7* RNA expression levels are shown (n = 6 subjects per group). (B) *RAB7* RNA expression was measured using qRT-PCR. The bar graph shows the fold change by ΔΔCT-method (n = 3 subjects/group, ns). (C) Western blots (used in Figure 5A) were stripped and re-probed to detect RAB7 protein expression levels. Position of RAB7 is marked. Corresponding ACTB loading control is shown at the bottom (same as shown in Figure **5A**) and was used for normalization of data presented in bar graph below. This figure is representative of n = 6 independent experiments. Significance is indicated by exact p-value where statistically significant.

(mitogen-activated protein kinase 1)/ERK2-MAPK3 (mitogen-activated protein kinase 3)/ERK1 and MTOR (Figures S4A-B), which are part of the previously characterized TLR4-MYD88 (MYD88 innate immune signal transduction adaptor)-MAP2K (mitogen-activated protein kinase kinase)/MEK-MAPK/ERK-MTOR pathway [57,58], known to be present and active in MKs and platelets [59–63].

To determine whether these *in vitro* responses in human cells were conserved *in vivo*, and to provide further mechanistic evidence, we also examined whether TLR4 regulated phosphorylation of MAPK1-MAPK3 and MTOR in platelets during experimental sepsis. As shown in Figures S4C-D, phosphorylation of MAPK1-MAPK3 and MTOR in platelets during endotoxemia sepsis was significantly reduced when TLR4 was pharmacologically inhibited.

RAB7 protein expression levels are reduced in human platelets under septic conditions

Next, we examined RAB7 expression levels. RAB7 is a small GTPase that controls transport to late endocytic compartments, including late endosomes and lysosomes [64]. In addition, RAB7 is a direct interaction partner of EPG5 in lysosomes [14]. *RAB7* mRNA expression was not significantly changed in platelets from septic patients, compared to healthy donors (Figure 6A and B). RAB7 protein levels were significantly reduced in platelets from septic patients (Figure 6C). Similar, but not significant, patterns were observed when late stages of autophagic flux were inhibited with bafilomycin A_1 (Figure 6C). These data demonstrate that reduced EPG5-LC3 interactions and decreased RAB7 expression levels characterize platelets isolated from septic patients.

Discussion

While platelets are anucleate cells with a short life-span (~10 days) they contain abundant mRNA [65,66], miRNA [67], and organelles, and use intricate regulatory pathways to fulfill their biologic tasks [48,49,52,54,68–72]. Research efforts in recent years revealed that platelets are not limited to hemostasis and thrombus formation, but also function as key immunologic cells in host defense [37,73,74] and the orchestration of inflammatory processes [32,34–36,75,76]. Platelets have been studied for vesicle trafficking, demonstrating that they contain all the necessary factors to perform autophagy [38,42]. Furthermore, those studies underscored the importance of autophagy for megakaryopoiesis, thrombopoiesis and platelet function [40,41,61,77]. Nevertheless, there is a paucity of data helping to understand platelet autophagy under inflammatory conditions.

Here, we demonstrate for the first time, to the best of our knowledge, that late-stage inhibition of autophagy, observed in platelets isolated from a Vici syndrome patient, also occurs in platelets from septic patients (Figure 3C, 5D, and 7). EPG5 protein expression level and its functionality were found to be decreased in a Vici syndrome patient due to the homozygous mutation (Table 1). Platelets isolated from septic patients also demonstrate decreased LC3 recognition and binding of EPG5 (Figure 5D), while providing evidence of EPG5-LC3 interactions [14] in human platelets under healthy conditions. In addition, using human MK cells, we were able to demonstrate that this process is dependent on TLR4 signaling (Figure 5E).

Our analyses of Vici syndrome patient platelets are also the first to examine these anucleate cells in this extremely rare patient population. Using microscopy techniques, the accumulation of autophagic vacuoles in various tissues was previously described as a hallmark finding in several Vici

syndrome patients [78–81]. Consistent with these findings we observed accumulation of LC3-positive particles in platelets isolated from the Vici syndrome patient. This not only suggests that the number of autophagosomes is increased in platelets, but also a failure to clear late-stage autophagosomes. These observations suggest that platelets are similarly affected by the defect in autophagy induced by *EPG5* mutations as are other tissues [15]. The clinically performed genetic sequencing of the Vici syndrome patient did demonstrate a deletion of thymidine in position 2,066, resulting in a non-sense frameshift. In concordance with this mutation, we were able to show decreased EPG5 protein expression levels (Figure 1E). In addition, based on the mutation-induced disturbed EPG5 function, we discovered that LC3 accumulates intracellularly and that protein levels of SQSTM1 increase in Vici syndrome patient platelets (Figure 1C D and), correlating with disturbed autophagic flux in affected cells [82]. Expression levels of corresponding transcripts could not be analyzed due to limited sample availability. Taken together, these clinically relevant molecular findings in the Vici syndrome patient, a patient population prone to immune-system disturbances, raised the question regarding whether altered autophagic function would be caused in platelets exposed to systemic inflammatory conditions.

Because of its clinical relevance, we decided to study platelet EPG5 function in a common, morbid, and often fatal systemic inflammatory disease – sepsis. Preliminary experiments performed in our laboratory (data not shown) paralleled the Vici syndrome platelet phenotype, demonstrating accumulation of vesicles in platelets isolated from patients with sepsis. The morphologic changes included the increased intracellular localization of LC3 positive particles (Figure 2C), and the accretion of vesicles, demarcated by a double membrane (hallmark of autophagosomes), visible on an ultrastructural level (Figure 2A). Some of these vesicles did contain organelles, i.e., mitochondria, indicative of selective mitophagy. In addition, the use of bafilomycin A_1, a vacuolar-type H^+-ATPase (V-ATPase) inhibitor, which blocks fusion of autophagosomes with lysosomes (late-stage inhibitor), reproduced the increased intracellular localization of LC3-positive structures in platelets from healthy individuals when compared to platelets from septic patients (Figure S2). Based on these observations, we conclude that autophagosomes, but not late degenerative autophagic vacuoles/autolysosomes (characterized by a single membrane), build up intracellularly in septic platelets. These findings did point toward a potential late-stage inhibition of the autophagic flux occurring in septic platelets.

Autophagosome evolution involves fusion with early and late endosomes [18], a sequence of events defining the maturation of autophagosomes and building the late-stage of autophagy. Published studies indicate that the fusion between autophagosome and lysosomes in mammalian cells is an intricate multi-step process regulated through complex molecular machinery [83]. The monitoring of autophagic flux using microscopy or flow cytometry approaches usually requires that the cells of interest are transfected with specific reporter constructs [44]. However, it is difficult to produce transfected and genetically modified uniform, high-quality human platelets. Therefore, a western blot-based approach was utilized. SQSTM1 and related LC3 binding protein turnover can be used as an index of autophagic turnover and degradation [44,47]. Our studies demonstrate increased levels of SQSTM1 in platelets isolated from septic patients when compared to healthy control donors (Figure 3). Treatment of healthy platelets with rapamycin (inducer of autophagy) resulted in increased autophagic flux, demonstrating the general ability of platelets to appropriately react to additional autophagic stimuli. In contrast, when comparing septic platelets treated with or without rapamycin with healthy platelets treated in similar fashion, we detected evidence of late-stage autophagic inhibition and decreased reactivity to pharmacologic stimuli. This finding is remarkable in the context of previously described dynamics of the autophagic system in clinical and experimental settings of sepsis. CLP-induced sepsis did result in initial clearance of autophagosomes, but accumulation of SQSTM1 at later stages of the disease (8 h) [21,23]. In addition, TEM analysis of tissues from septic animals did reveal an increased number of autophagosomes, but only few autolysosomes [27], also supporting the hypothesis of reduced autophagosomal and lysosomal fusion. Furthermore, using a CLP mouse model utilizing platelet specific *mtor* knockout (KO) animals, we were able to recapitulate the accumulation of autophagosomes in platelets isolated from mice exposed to the inflammatory condition (Figure S5). While the knockdown of MTOR will result in increased autophagic activity (paralleling the effects of the pharmacological inhibitor of MTOR, rapamycin), these preliminary animal model results indicate similar autophagic mechanisms are active in this sepsis model. This will enable us to study the molecular mechanisms described in this study in more detail using future animal model approaches.

The RAB-SNARE system has been demonstrated to be play a crucial role in the autophagosome-lysosome fusion process [84]. However, the interacting molecules embedded in the autophagosomal and lysosomal membrane and potential adapter molecules were only recently identified. Experimental studies utilizing Vici-syndrome patient samples demonstrated that EPG5 was recruited to late endosomes/lysosomes by RAB7, and tethering of this complex to autophagosomes by EPG5-LC3 interaction leads to maturation of autolysosomes [14]. Therefore, we analyzed the changes of transcripts essential for autophagy and autophagosome-lysosome fusion in human platelets. The detected decrease in *EPG5* expression levels in platelets isolated from septic patients did further point toward a disturbance of the autophagosome-lysosome fusion process. In contrast to the mRNA expression levels, our protein expression analysis of EPG5 and LC3 did demonstrate increased amounts of those proteins in septic platelets, suggesting abundant presence of such critical proteins. Findings of contrasting mRNA and protein expression dynamics are not unusual, and were described before [51]. These discrepancies in mRNA and protein expression levels are reflective of a megakaryocyte driven selective transfer (i.e. influenced by external inflammatory cues), rather than randomly dispensed mRNAs and proteins into platelets. Furthermore, translational control mechanisms and changes in RNA stability can be responsible for differences in RNA and protein expression levels.

Induction of autophagy in healthy control platelets resulted in increased direct EPG5-LC3 interaction (Figure 5D), potentially indicating increased fusion of autophagosomes with late endosomes/lysosomes [14]. In contrast, septic platelets revealed reduced EPG5-LC3 interaction (Figure 5D and Figure S3). These findings are indicative of late-stage inhibition of autophagy due to reduced EPG5-LC3 guided autophagosome-lysosome fusion in human platelets isolated from septic patients, despite increased total EPG5 and LC3 protein levels. This is the first time that late-stage inhibition due to diminished EPG5-LC3 interaction guided autophagosome-lysosome fusion is implicated in platelet function in human sepsis. We [48,50] and others [85,86] have previously reported that during sepsis, platelets demonstrate increased surface expression of SELP (selectin P; secreted by alpha-granules), and greater activation of integrin αIIbβ3 on the platelet surface, thereby enhancing platelet aggregation. Autophagy regulates many aspects of cell secretory events [87] and, while our study did not permit us to perform associative analyses between platelet activation responses and autophagy, Ouseph and colleagues have reported that autophagic pathways in non-septic platelets control granule secretion and aggregation [41] (also reviewed in [88]).

Other investigators have demonstrated that accumulation of autophagosomes induces cellular toxicity [89]. This disruption of autophagic flux was also shown to have pathologic relevance most notably when combining chemotherapeutic drugs with autophagosome clearance inhibitors in tumor studies [90]. While the induction of increased cell death is beneficial in the setting of cancer therapy, it was demonstrated that decreased numbers of circulating platelets were linked to increased patient mortality during sepsis [91] (and reviewed in [92]). Therefore, based on our results, altered autophagic flux in human platelets could be added to the growing list of thrombocytopenia-inducing mechanisms during sepsis associated with adverse outcomes [92], and may offer new therapeutic avenues.

We also demonstrate decreased RAB7 protein expression in septic platelets (Figure 6C). RAB7 is expressed on the surface of late endosomes/lysosomes [93], and was shown to be affected by EPG5. EPG5-RAB7 interactions, in concert with LC3 binding, was demonstrated to determine the fusion specificity of autophagosomes and with late endosomes/lysosomes [14,64,94]. The decreased expression of RAB7 might be an integral part of the dysregulated autophagic flux we observed in septic platelets and could contribute to the detected late-stage inhibition. Future studies centered around RAB7 in platelets may add another facet to the multifactorial dysfunction of autophagy under septic conditions detected in human platelets.

Finally, to further decipher the signaling mechanism involved in diminished EPG5-LC3 interaction, we utilized a well-established platelet-surrogate MK culture model, as previously used by our laboratory [37,52–54]. LPS is one of the major determinants in gram-negative sepsis [95]. LPS is a ligand of TLR4, which is expressed by $CD34^{+}$-derived MKs [96]. Engagement of TLR4 by LPS triggers dimerization and association of MYD88 with the intracellular TIR (Toll/IL-1 receptor) domain of TLR4, or TRIF-dependent signaling, followed by additional signal transduction events [97,98]. We found that a well-characterized small molecule inhibitor that selectively blocks TLR4 signaling (CLI-095) restored the diminished EPG5-LC3 protein-protein interaction (Figure 5E). Taken together, these results suggest that in our model-cell system of MKs and their daughter cells, human platelets, sepsis-induced dysregulated autophagy, and EPG5-LC3 disengagement, are mediated by LPS-signaling through TLR4. This novel finding expands on the linkage of LPS and autophagy [99]. Additional downstream signaling intermediates are active in MKs and human platelets [59–63], directly linking TLR4 to autophagy, as the TLR4-MYD88-MAP2K/MEK-MAPK/ERK-MTOR pathway [57] demonstrated increased phosphorylation events under simulated septic conditions and in murine models of sepsis due to endotoxemia (Figure S4). These findings warrant further investigation in future studies.

Our experimental approach for this study was driven by the guidelines for autophagy research [44]. Nevertheless, there are some limitations to this study. First, we were only able to study autophagy in platelets from one patient with Vici syndrome. However, this syndrome is extremely rare, and only ~78 patients have been reported in the literature [17] since its first description in 1988 [100]. The median survival of most patients with Vici syndrome is also only 42 months from birth. This makes studying patients with Vici syndrome exceedingly difficult. We also appreciate that our cohort of septic patients and healthy donors were not specifically age-matched and that sepsis has heterogenous clinical features (as shown in Table 3). We appreciate that while matched on the variable of sex, health donors and septic patients were not matched on the variable of age. Nevertheless, we did not identify any significant differences between younger and older subjects with regards to platelet autophagosome content, autophagic flux, or EPG5 levels. Therefore, we do not believe age represents a significant confounder for our study. In exploratory analyses, we also did not find any significant associations between clinical features of sepsis and alterations in platelet autophagy. Finally, we recognize that our clinical and *in vitro* findings might be extended in future studies by *in vivo* work using relevant mouse models where *Epg5* is genetically altered in platelets and megakaryocytes. These murine models currently do not exist, and may be the focus of future studies.

In conclusion, our data identify a previously unrecognized regulatory mechanism of autophagy as present in human platelets. Our findings demonstrate that during sepsis, RAB7 (an integral protein to coordinate the autophagosome-lysosome fusion process) in platelets is decreased. Together, these are associated with reduced platelet autophagy activity. Finally, we propose that under septic conditions, the maturation of autolysosomes is disturbed due to LPS-TLR4 signaling and diminished interactions of EPG5 and LC3. This mimics aspects of the molecular base of the late-stage autophagy inhibition described in Vici syndrome patients (Figure 7).

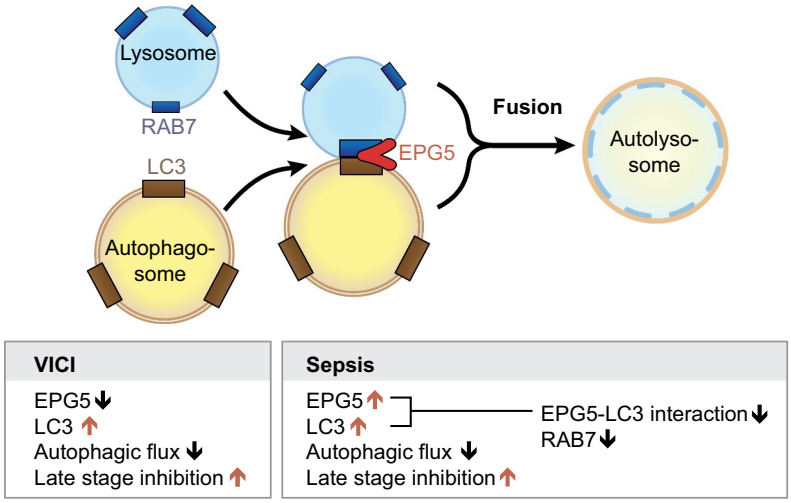

Figure 7. Sepsis induces TLR-4 dependent dysregulation of EPG5-LC3 protein-protein interaction resulting in decreased autophagic flux and late-stage inhibition. Model showing how EPG5 mediates fusion of autophagosomes with lysosomes. EPG5 is recruited to lysosomes by associating with RAB7 and LC3. Left box summarizes know autophagic determinates from the literature and our findings for Vici-patient. The right box synopsizes our experimental findings in septic patients, making comparisons between patients with Vici syndrome and sepsis where possible.

Materials and Methods

Vici syndrome patient

Patient was identified based on characteristics listed in Table 1.

Septic patients and Healthy Controls

Patients were selected for meeting consensus criteria for sepsis [101], enrolled within 48 h of ICU admission, and demonstrated demographic and clinical characteristics as outlined in Table 2. Healthy controls were sex-matched to septic patients and their demographics are shown in Table 3.

Reagents and antibodies

The following drugs and reagents were used freshly prepared or from stock solutions: rapamycin (200 nM; Millipore Sigma, 553,210), bafilomycin A_1 (200 nM; Millipore Sigma, 196,000), CLI-095 (1 μM; InvivoGen, Tlrl-cli95), and LPS (100 ng/mL; Millipore Sigma, L6011). The following reagents and antibodies were used for microscopy, western blot, and co-IP studies as described below: Paraformaldehyde (PFA 4% [2% final]), Alexa Fluor® 555 or 633 conjugate of wheat germ agglutinin (WGA, 1:1000; Thermo Fisher Scientific, W32464, W21404), rabbit anti-LC3B antibody (abcam, ab48394), mouse anti-LC3B (abcam, ab243506), mouse anti-SQSTM1/p62 antibody (abcam, ab56416). A rabbit anti-EPG5 (Thermo Fisher Scientific, PA5-38,062; and LifeSpan, C413653), mouse anti-ACTB/actin HRP-conjugated (abcam, ab20272), mouse anti-LAMP1 (abcam, ab25630), mouse anti-RAB7 (abcam, ab50533), rabbit anti-MAPK1/ERK2-MAPK3/ERK1, rabbit anti-MAPK1/ERK2-MAPK3/ERK1 Tyr202/Tyr204, rabbit anti-MAPK/p38, rabbit anti-MAPK/p38 Tyr180/Tyr182, rabbit anti-MTOR, rabbit anti-MTOR Ser2448 (all Cell Signaling Technology, 9102, 9101, 9212, 9211, 2971, 2971S). Secondary biotinylated or HRP-conjugated antibodies, and streptavidin Alexa Fluor® purchased from Thermo Fisher Scientific (31,424, 31,864, 31,452, A16170, S11223, S32355).

Platelet isolation and culture

All studies were approved by the institutional ethics committee (IRB#000392 and IRB#00046263). Platelets used for the described studies were freshly isolated from septic patients and gender-matched, medication-free, healthy human subjects. In select studies, platelets were isolated from a pediatric patient diagnosed with Vici Syndrome, and gender-matched, medication-free, healthy individual. Platelets were leukocyte-reduced and isolated as previously described to yield a highly-purified population of cells with <1 leukocyte per 10^7 platelets [52,54,69]. Depleted platelets were resuspended at $1x10^8$/mL in serum-free M199 medium (Thermo Fisher Scientific, 11,150,067), placed in round-bottom polypropylene tubes, and incubated, where indicated, in a 37°C humidified incubator at 5% CO_2 for different time points. In select studies, platelets were treated (2 h) with rapamycin, bafilomycin A_1 or its vehicle control (DMSO).

$CD34^+$-derived megakaryocytes (MKs)

$CD34^+$ hematopoietic progenitor cells were isolated from human umbilical cord blood and differentiated into proplatelet-producing MKs as previously described [52–54]. Minor changes in protocol were implemented. In brief, StemSpan SFEM II media (Stemcell Technologies, 09655) was used for

standard culture conditions. On day 10, some cells were treated with CLI-095 (1 μM), and/or with LPS (100 ng/mL).

Immunocytochemistry

Freshly isolated platelets were fixed in suspension using PFA, permeabilized with 0.1% Triton X-100 (Thermo Fisher Scientific, AC327372500) for 5 min at room temperature (RT) and subsequently layered onto VECTABOND™ (Vector Laboratories, SP1800) coated coverslips using a cytospin centrifuge (Shandon Cytospin, Thermo Fisher Scientific, Waltham, MA, USA). Cells were incubated with IgG (to control for specificity of signal) or an antibody against targets as listed above (see reagents and antibodies paragraph) overnight at 4°C. Cells were subsequently incubated with secondary biotinylated antibodies, and signals were amplified using streptavidin Alexa Fluor® 488 or 546. Sialic acids/glycoproteins (in cell membranes/granular content) and the actin cytoskeleton were co-stained using WGA or phalloidin (Thermo Fisher Scientific, W32464, W21404, A12379, A22283), respectively.

Microscopy and image analysis

Fluorescence microscopy and high-resolution confocal reflection microscopy were performed using an Olympus IX81, FV300 (Olympus, Melville, NY) confocal-scanning microscope equipped with a 60x/1.42 NA oil objective for viewing platelets. An Olympus FVS-PSU/IX2-UCB camera and scanning unit and Olympus Fluoview FV 300 image acquisition software version 5.0 were used for recording. Monochrome 16-bit images were further analyzed and changes quantified using Adobe Photoshop CS6, ImageJ (NIH), and CellProfiler (www.cellprofiler.org) with a custom analysis set *[102]. In brief, raw images with visible signal for IgG background were automatically analyzed to minimize observer bias. While this might lead to increased signal intensity across all samples (Figure 5B), the introduction of threshold parameters adjusts for visible IgG staining in the analysis set (Figure 5C). The following software parameters were introduced: threshold method – otsu (this approach calculates the threshold separating three classes of pixels by minimizing the variance within each class); threshold correction factor – 2.5 (a value > 1 makes the threshold more stringent, since the otsu method will give a slightly biased threshold if a larger percentage of the image is covered with positive signal).*

Protein expression studies

All samples were normalized for starting cell concentrations. Platelets were lysed in Laemmli-buffer, and samples were separated by SDS-polyacrylamide gel electrophoresis (SDS-PAGE) and examined by western analysis for LC3, SQSTM1/p62, EPG5, RAB7, MAPK1-MAPK3, MAPK/p38, and MTOR expression patterns. Subsequently, proteins were detected by enhanced chemiluminescence (ECL; Thermo Fisher Scientific, 32,132). Linear range of detection was assured by using the saturation detection mode of the myECL Imager (Thermo Fisher Scientific, Waltham, MA, USA). Specific protein expression was normalized using ACTB/actin expression and quantified using ImageJ (NIH).

Transmission electron microscopy

For the ultrastructural analyses, platelets were spun down on acylar disks coated with poly-L-lysine (Thermo Fisher Scientific, P8920), fixed in 4% formaldehyde, 1% glutaraldehyde (Electron Microscopy Sciences, 16,536–05) in 0.1 M phosphate-buffered saline (PBS; 80.0 g NaCl, 2.0 g KCl, 21.7 g Na_2HPO_4 $7H_2O$, 2.59 g KH_2PO_4, fill up to 1.0 L ddH_2O, adjust to pH 7.4) overnight. Platelets were washed with 0.1 M phosphate buffer (pH 7.4), followed by distilled H_2O. Platelets were then post-fixed with 2% osmium tetroxide (60 min), washed twice with distilled H_2O, dehydrated by a graded series of acetone concentrations (50%, 70%, 90%, and 100%; 2 × 10 min each) followed by embedding in Epon (Millipore Sigma, 45,345). Thin sections were examined with a JEOL JEM-1400 electron microscope (JEOL, Peabody, MA, USA), after uranyl acetate and lead citrate staining. Digital images were captured with a side-mounted Advantage HR CCD camera (Advanced Microscopy Techniques, Woburn, MA, USA), saved in TIFF format, and trimmed for publication using Adobe Photoshop CS6. Autophagosomes were assessed and counted in a blinded fashion.

Super-resolution microscopy

Using this technique, two-point sources closer than the width of their point source function can be distinguished. Having only a few labeling molecules in a fluorescent state (blinking function) at any time allows the location of each molecule to be individually determined with high precision [103–105]. Therefore, this technique is primarily aimed at defining a location instead of intensity of fluorophore. Platelets were pretreated with rapamycin or bafilomycin A_1 as aforementioned. Cells were fixed in suspension using paraformaldehyde (PFA, 2% final concentration). The fixed cells were spun down onto poly-L-lysine-coated chamber slides using standard centrifugation, and custom slide holder. Cells were washed (HBSS, 3x), and permeabilized using HBSS 0.1% Triton X-100 for 5 min. Cells were washed (HBSS, 3x), and nonspecific binding blocked using HBSS containing filtered donkey serum (10%; abcam, ab7475) for 1 h. at room temperature. Cells were subsequently incubated with primary antibodies (rabbit anti-LC3 antibody, and mouse anti-LAMP1) at 4°C overnight. Next, samples were incubated with secondary antibodies: goat anti-rabbit Alexa Fluor 647, and donkey anti-mouse Cy3b (1:1,000, 1 h at RT, in-house custom labeling). After additional washing steps, cells were post-fixed using 4% paraformaldehyde for 10 min at RT. Samples were imaged using a Bruker Vutara SR200 Biplane 3D microscope (Bruker, Middleton, WI, USA) equipped for single molecule localization microscopy (SMLM). Images were analyzed using the proprietary software, Vutara SRX software, and results transferred to Adobe Photoshop CS6, and ImageJ (NIH).

Autophagic flux evaluation

Platelets were treated with rapamycin, bafilomycin A_1 or its vehicle control (DMSO). Platelets were lysed in Laemmli-buffer, and samples were separated by SDS-polyacrylamide gel electrophoresis (SDS-PAGE) and examined by western analysis for LC3, and SQSTM1/p62 expression pattern. Proteins were detected by enhanced chemiluminescence (ECL). Specific protein expression was normalized using ACTB/actin expression and quantified using ImageJ (NIH). Resulting data were interpreted as previously described [47,106,107]. In brief, an increase in the levels of LC3-II observed under septic conditions in the presence of bafilomycin A_1, compared with the treatment alone, is indicative of some degree of flux in the cell system used. However, a condition increasing LC3-II on its own that has no difference in LC3-II in the presence of bafilomycin A_1 compared with treatment alone may suggest a block in autophagy at the terminal stages [44,47].

RNA isolation

Platelets were lysed in TRIzol (Thermo Fisher Scientific, 15,596,026), and RNA isolation was performed as previously described [52,54].

Next generation RNA-sequencing

For next-generation RNA-sequencing (RNA-seq), 1×10^9 isolated platelets were carefully lysed in TRIzol and DNase treated. Total RNA was isolated, as previously described [48,53,65,67,108]. An Agilent bio-analyzer 2100 (Agilent, Santa Clara, CA, USA) was used to quantify the amount and quality of the total RNA. RNA Integrity Number (RIN) scores were similar between all samples. RNA-seq libraries were prepared with TruSeq V2 with oligo-dT selection (Illumina, RS-122-2001). Reads were aligned (Novoalign) to the reference genome at the time of these studies (GRCh37/hg19) and a pseudo-transcriptome containing splice junctions. The Deseq2 analysis package was used to assign reads to composite transcripts (one per gene) and quantitate fragments per kilobase of transcript per million mapped reads/FPKMs. Gene expression was considered significantly differentially expressed if the false discovery rate was <0.05 and the $\log_2$ fold change was ≥ 1.5.

PCR and real-time qPCR studies

To determine *EPG5* and *RAB7* mRNA expression pattern in human platelets, primers flanking *EPG5* (5′-AACAGGT CACCCACAAGGTG-3′ and 5′- GGGTAACCCATA CTGTGGTC-3′) and *RAB7* (5′-GTTCCAGTCTCTCGGT GTGG-3′ and 5′- AAGTGCATTCCGTGCAATCG-3′) were used (in-house synthesis) and PCR was performed. mRNA expression was detected by qRT-PCR (iCycler, Bio-Rad, Hercules, CA, USA), and expression levels were calculated using the ΔΔCT method.

Co-immunoprecipitation *studies*

For all modified protein Co-IP studies, the Magna RIP RNA-binding protein immunoprecipitation kit (Millipore Sigma, 17–700) was used according to the manufacturer's protocol. In brief, 2×10^9 total platelets were first lysed in 400 µl of complete RIP lysis buffer. Next, lysates from 0.5×10^9 platelets or MKs were used in each reaction. The magnetic beads used for the IP reaction were either incubated with the antibody of interest (anti-LC3) or the respective IgG control for 30 min at RT. Co-IP was performed using the prepared beads, the supplied buffer and 100 µl of the platelet cell lysate with constant rotation overnight at 4°C. Beads were washed the next days (x6), immobilized on a magnet, and the proteins were eluted using Laemmli-buffer. Proteins were separated using SDS-PAGE and western blot techniques as described above.

Proximity Localization Assay colocalization studies (PLA)

Microscopy-based single recognition and colocalization studies were performed as previously described [53] using the Duolink® in situ system (Millipore Sigma). In brief, unique short DNA strands attached to secondary antibodies against a single or two target proteins (PLA (+) and (−) probes) bind to the primary antibodies. The oligonucleotides guide the formation of circular DNA strands when bound in close proximity (< 40 nm). The DNA circles serve as templates for localized rolling-circle amplification, allowing individual interacting pairs of protein molecules to be visualized by additional hybridization techniques [109]. Platelets were isolated, fixed in suspension with paraformaldehyde (2% final) and permeabilized for microscopy as described above. The Duolink in situ kit was used as recommended by the manufacturer with the primary antibodies rabbit anti-EPG5 and mouse anti-LC3B. One primary antibody was omitted or nonimmune IgGs were used as negative controls. Secondary anti-mouse (+) or (−) and anti-rabbit (+) or (−) antibodies were used as PLA probes. After hybridization, ligation and amplification, a detection solution containing fluorescent probes was added. PLA signals were then detected by confocal microscopy as described above.

Murine endotoxemia studies

Animal studies were approved by the University of Utah Institutional Animal Care and Use Committee (18–10,012). C57BL6/J mice were purchased from Jackson Laboratory (8- to 12-weeks old). Endotoxemia was induced in mice using by i.p. injections of LPS from *Escherichia coli* O55:B5 (5 mg/kg; Sigma-Aldrich, L6529). Mice were pretreated with TAK-242 (3 mg/kg; Tocris, 6587/5), a specific TLR4 inhibitor [110,111], or vehicle control (PBS containing 0.9% DMSO) by i.v. injections 1 h before LPS treatment. After 24 h, platelets were isolated as described above and probed for total and phosphorylated MTOR and MAPK1-MAPK3.

Statistical analyses

The mean±SEM was determined for each variable. Student t-tests or ANOVA (where multiple groups were compared) was used to identify differences among two or multiple experimental groups respectively (GraphPad Prism v7.0). If significant differences were found, a Newman-Keuls post-hoc analysis was used to determine the location of the difference (applicable for ANOVA). Basic science data were also examined for normality using skewness and kurtosis tests. Non-parametric distribution was detected for data presented in Figure 2B, and data was analyzed using Wilcoxon Signed Rank test. For all analyses, p-value <0.05 was considered significant, and exact p-values are indicated for each figure if significance was detected.

Acknowledgments

We thank Chris K. Rodesch and Keith R. Carney of the University of Utah Cell Imaging Core, Linda Nikolova of the University of Utah Electron Microscopy Core, and Manasa V. Gudheti of the Department of Biology for technical assistance. We also thank Diana Lim for preparation of the figures, critical comments, and consultation regarding effective display of the images.

Disclosure statement

No potential conflict of interest was reported by the author(s).

Funding

This work was supported by the National Institutes of Health (R01HL142804, R01AG048022, R56AG059877, and R01HL130541 to M.T. Rondina, K01AG059892 to R.A. Campbell, K08HL153953 to E.A. Middleton, R01HL144957 to J.W. Rowley), and the University of Utah Triple I Program (E.A. Middelton). This work was also supported, in part, by Merit Review Award Number I01 CX001696 to M.T. Rondina from the US Department of Veterans Affairs Clinical Sciences R&D. This material is the result of work supported with resources and the use of facilities at the George E. Wahlen VA Medical Center, Salt Lake City, Utah. The contents do not represent the views of the US Department of Veterans Affairs or the US Government.

References

[1] Pool R, Gomez H, Kellum JA. Mechanisms of Organ Dysfunction in Sepsis. Critical Care Clinics. 2018;34(1):63–80.
[2] Xiao W, Mindrinos MN, Seok J, et al. A genomic storm in critically injured humans. J Exp Med. 2011;208(13):2581–2590.
[3] Hotchkiss RS, Karl IE. The pathophysiology and treatment of sepsis. N Engl J Med. 2003;348(2):138–150.
[4] Hotchkiss RS, Nicholson DW. Apoptosis and caspases regulate death and inflammation in sepsis. Nat Rev Immunol. 2006;6(11):813–822.
[5] Dalager-Pedersen M, Sogaard M, Schonheyder HC, et al. Risk for myocardial infarction and stroke after community-acquired bacteremia: a 20-year population-based cohort study. Circulation. 2014;129(13):1387–1396.
[6] Kaplan D, Casper TC, Elliott CG, et al. VTE Incidence and Risk Factors in Patients With Severe Sepsis and Septic Shock. Chest. 2015;148(5):1224–1230.
[7] Smeeth L, Thomas SL, Hall AJ, et al. Risk of myocardial infarction and stroke after acute infection or vaccination. N Engl J Med. 2004;351(25):2611–2618.
[8] Bento CF, Renna M, Ghislat G, et al. Mammalian Autophagy: how Does It Work? Annu Rev Biochem. 2016;85(1):685–713.
[9] Shaid S, Brandts CH, Serve H, et al. Ubiquitination and selective autophagy. Cell Death Differ. 2013;20(1):21–30.
[10] Zaffagnini G, Martens S. Mechanisms of Selective Autophagy. J Mol Biol. 2016;428(9):1714–1724.
[11] Hurley JH, Young LN. Mechanisms of Autophagy Initiation. Annu Rev Biochem. 2017;86(1):225–244.
[12] Feng Y, He D, Yao Z, et al. The machinery of macroautophagy. Cell Res. 2014;24(1):24–41.
[13] Suzuki H, Osawa T, Fujioka Y, et al. Structural biology of the core autophagy machinery. Curr Opin Struct Biol. 2017;43:10–17.
[14] Wang Z, Miao G, Xue X, et al. The Vici Syndrome Protein EPG5 Is a Rab7 Effector that Determines the Fusion Specificity of Autophagosomes with Late Endosomes/Lysosomes. Mol Cell. 2016;63(5):781–795.
[15] Byrne S, Dionisi-Vici C, Smith L, et al. Vici syndrome: a review. Orphanet J Rare Dis. 2016;11(1):21.
[16] Zhao YG, Zhao H, Sun H, et al. Role of Epg5 in selective neurodegeneration and Vici syndrome. Autophagy. 2013;9(8):1258–1262.
[17] Alzahrani A, Alghamdi AA, Waggass R. A Saudi Infant with Vici Syndrome: case Report and Literature Review. Open Access Maced J Med Sci. 2018;6(6):1081–1084.
[18] Lamb CA, Dooley HC, Tooze SA. Endocytosis and autophagy: shared machinery for degradation. Bioessays. 2013;35(1):34–45.
[19] Ho J, Yu J, Wong SH, et al. Autophagy in sepsis: degradation into exhaustion? Autophagy. 2016;12(7):1073–1082.
[20] Schmid D, Munz C. Innate and adaptive immunity through autophagy. Immunity. 2007;27(1):11–21.
[21] Takahashi W, Watanabe E, Fujimura L, et al. Kinetics and protective role of autophagy in a mouse cecal ligation and puncture-induced sepsis. Crit Care. 2013;17(4):R160.
[22] Feng Y, Liu B, Zheng X, et al. The protective role of autophagy in sepsis. Microb Pathog. 2019;131:106–111.
[23] Lin C-W, Lo S, Perng D-S, et al. Complete activation of autophagic process attenuates liver injury and improves survival in septic mice. Shock. 2014;41(3):241–249.
[24] Chien W-S, Chen Y-H, Chiang P-C, et al. Suppression of autophagy in rat liver at late stage of polymicrobial sepsis. Shock. 2011;35(5):506–511.
[25] Zhang L, Ai Y, Tsung A. Clinical application: restoration of immune homeostasis by autophagy as a potential therapeutic target in sepsis. Exp Ther Med. 2016;11(4):1159–1167.
[26] Lo S, Yuan S-SF, Hsu C, et al. Lc3 over-expression improves survival and attenuates lung injury through increasing autophagosomal clearance in septic mice. Ann Surg. 2013;257(2):352–363.
[27] Hsieh C-H, Pai P-Y, Hsueh H-W, et al. Complete induction of autophagy is essential for cardioprotection in sepsis. Ann Surg. 2011;253(6):1190–1200.
[28] Rondina Mt, Carlisle M, Fraughton T, et al. Platelet-monocyte aggregate formation and mortality risk in older patients with severe sepsis and septic shock. J Gerontol A Biol Sci Med Sci. 2015;70(2):225–231.
[29] Venkata C, Kashyap R, Farmer JC, et al. Thrombocytopenia in adult patients with sepsis: incidence, risk factors, and its association with clinical outcome. J Intensive Care. 2013;1(1):9.
[30] Yaguchi A, Lobo FL, Vincent J-L, et al. Platelet function in sepsis. J Thromb Haemost. 2004;2(12):2096–2102.
[31] Hamzeh-Cognasse H, Damien P, Chabert A, et al. Platelets and Infections â€“ Complex Interactions with Bacteria. Front Immunol. 2015;6:82.
[32] Semple JW, Italiano JE Jr., Freedman J. Platelets and the immune continuum. Nat Rev Immunol. 2011;11(4):264–274.
[33] Vieira-de-Abreu A, Campbell RA, Weyrich AS, et al. Platelets: versatile effector cells in hemostasis, inflammation, and the immune continuum. Semin Immunopathol. 2012;34:5–30.
[34] Weyrich AS, Lindemann S, Zimmerman GA. The evolving role of platelets in inflammation. J Thromb Haemost. 2003;1(9):1897–1905.

[35] Weyrich AS, Zimmerman GA. Platelets: signaling cells in the immune continuum. Trends Immunol. 2004;25(9):489–495.
[36] Campbell RA, Franks Z, Bhatnagar A, et al. Granzyme A in Human Platelets Regulates the Synthesis of Proinflammatory Cytokines by Monocytes in Aging. J Immunol. 2018;200(1):295–304.
[37] Campbell RA, Schwertz H, Hottz ED, et al. Human megakaryocytes possess intrinsic antiviral immunity through regulated induction of IFITM3. Blood. 2019;133(19):2013–2026.
[38] Feng W, Chang C, Luo D, et al. Dissection of autophagy in human platelets. Autophagy. 2014;10(4):642–651.
[39] Cao Y, Cai J, Zhang S, et al. Loss of autophagy leads to failure in megakaryopoiesis, megakaryocyte differentiation, and thrombopoiesis in mice. Exp Hematol. 2015;43(6):488–494.
[40] You T, Wang Q, Zhu L. Role of autophagy in megakaryocyte differentiation and platelet formation. Int J Physiol Pathophysiol Pharmacol. 2016;8:28–34.
[41] Ouseph MM, Huang Y, Banerjee M, et al. Autophagy is induced upon platelet activation and is essential for hemostasis and thrombosis. Blood. 2015;126(10):1224–1233.
[42] Luo X-L, Jiang J-Y, Huang Z, et al. Autophagic regulation of platelet biology. J Cell Physiol. 2019;234(9):14483–14488.
[43] Piano Mortari E, Folgiero V, Marcellini V, et al. The Vici syndrome protein EPG5 regulates intracellular nucleic acid trafficking linking autophagy to innate and adaptive immunity. Autophagy. 2018;14(1):22–37.
[44] Klionsky DJ, Abdelmohsen K, Abe A, et al. Guidelines for the use and interpretation of assays for monitoring autophagy (3rd edition). Autophagy. 2016;12:1–222.
[45] Li M, Khambu B, Zhang H, et al. Suppression of lysosome function induces autophagy via a feedback down-regulation of MTOR complex 1 (MTORC1) activity. J Biol Chem. 2013;288(50):35769–35780.
[46] Cullup T, Kho AL, Dionisi-Vici C, et al. Recessive mutations in EPG5 cause Vici syndrome, a multisystem disorder with defective autophagy. Nat Genet. 2013;45(1):83–87.
[47] Klionsky DJ, Abdalla FC, Abeliovich H, et al. Guidelines for the use and interpretation of assays for monitoring autophagy. Autophagy. 2012;8:445–544.
[48] Rondina MT, Schwertz H, Harris ES, et al. The septic milieu triggers expression of spliced tissue factor mRNA in human platelets. J Thromb Haemost. 2011;9(4):748–758.
[49] Schwertz H, Rowley JW, Schumann GG, et al. Endogenous LINE-1 (Long Interspersed Nuclear Element-1) Reverse Transcriptase Activity in Platelets Controls Translational Events Through RNA–DNA Hybrids. Arterioscler Thromb Vasc Biol. 2018;38(4):801–815.
[50] Middleton EA, Rowley JW, Campbell RA, et al. Sepsis alters the transcriptional and translational landscape of human and murine platelets. Blood. 2019;134(12):911–923.
[51] Cecchetti L, Tolley ND, Michetti N, et al. Megakaryocytes differentially sort mRNAs for matrix metalloproteinases and their inhibitors into platelets: a mechanism for regulating synthetic events. Blood. 2011;118(7):1903–1911.
[52] Denis MM, Tolley ND, Bunting M, et al. Escaping the nuclear confines: signal-dependent pre-mRNA splicing in anucleate platelets. Cell. 2005;122(3):379–391.
[53] Rondina MT, Freitag M, Pluthero FG, et al. Non-genomic activities of retinoic acid receptor alpha control actin cytoskeletal events in human platelets. J Thromb Haemost. 2016;14(5):1082–1094.
[54] Schwertz H, Tolley ND, Foulks JM, et al. Signal-dependent splicing of tissue factor pre-mRNA modulates the thrombogenecity of human platelets. J Exp Med. 2006;203(11):2433–2440.
[55] Manne BK, Bhatlekar S, Middleton EA, et al. Phospho-inositide-dependent kinase 1 regulates signal dependent translation in megakaryocytes and platelets. J Thromb Haemost. 2020;18(5):1183–1196.
[56] Kawamoto T, Ii M, Kitazaki T, et al. TAK-242 selectively suppresses Toll-like receptor 4-signaling mediated by the intracellular domain. Eur J Pharmacol. 2008;584(1):40–48.
[57] Yang J, Liu H, Han S, et al. Melatonin pretreatment alleviates renal ischemia-reperfusion injury by promoting autophagic flux via TLR4/MyD88/MEK/ERK/mTORC1 signaling. FASEB J. 2020;34(9):12324–12337.
[58] Zhou M, Xu W, Wang J, et al. Boosting mTOR-dependent autophagy via upstream TLR4-MyD88-MAPK signalling and downstream NF-κB pathway quenches intestinal inflammation and oxidative stress injury. EBioMedicine. 2018;35:345–360.
[59] Schattner M. Platelet TLR4 at the crossroads of thrombosis and the innate immune response. J Leukoc Biol. 2019;105(5):873–880.
[60] Severin S, Ghevaert C, Mazharian A. The mitogen-activated protein kinase signaling pathways: role in megakaryocyte differentiation. J Thromb Haemost. 2010;8(1):17–26.
[61] Wang Q, You T, Fan H, et al. Rapamycin and bafilomycin A1 alter autophagy and megakaryopoiesis. Platelets. 2017;28(1):82–89.
[62] Liu Z-J, Italiano J Jr., Ferrer-Marin F, et al. Developmental differences in megakaryocytopoiesis are associated with up-regulated TPO signaling through mTOR and elevated GATA-1 levels in neonatal megakaryocytes. Blood. 2011;117(15):4106–4117.
[63] Sun R-J, Shan -N-N. Megakaryocytic dysfunction in immune thrombocytopenia is linked to autophagy. Cancer Cell Int. 2019;19(1):59.
[64] Guerra F, Bucci C. Multiple Roles of the Small GTPase Rab7. Cells. 2016;5(3):34.
[65] Rowley JW, Oler AJ, Tolley ND, et al. Genome-wide RNA-seq analysis of human and mouse platelet transcriptomes. Blood. 2011;118(14):e101–11.
[66] Rowley JW, Schwertz H, Weyrich AS. Platelet mRNA: the meaning behind the message. Curr Opin Hematol. 2012;19(5):385–391.
[67] Rowley JW, Chappaz S, Corduan A, et al. Dicer1-mediated miRNA processing shapes the mRNA profile and function of murine platelets. Blood. 2016;127(14):1743–1751.
[68] Lindemann S, McIntyre TM, Prescott SM, et al. Platelet Signal-Dependent Protein Synthesis. In: Fitzgerald DJ, Quinn M, editors. Platelet Function: assessment, Diagnosis, and Treatment. Totowa: The Humana Press Inc; 2005. p. 151–176.
[69] Schwertz H, Koster S, Kahr WHA, et al. Anucleate platelets generate progeny. Blood. 2010;115(18):3801–3809.
[70] Schwertz H, Rondina MT. Platelets and their Microparticles go hand in hand. Thromb Res. 2018;168:164–165.
[71] Schwertz H, Rowley JW, Tolley ND, et al. Assessing protein synthesis by platelets. Methods Mol Biol. 2012;788:141–153.
[72] Schwertz H, Rowley JW, Zimmerman GA, et al. Retinoic acid receptor-α regulates synthetic events in human platelets. J Thromb Haemost. 2017;15(12):2408–2418.
[73] Kraemer BF, Campbell RA, Schwertz H, et al. Novel Anti-bacterial Activities of β-defensin 1 in Human Platelets: suppression of Pathogen Growth and Signaling of Neutrophil Extracellular Trap Formation. PLoS Pathog. 2011;7(11):e1002355.
[74] Rondina M, Garraud O, Schwertz H. Platelets and bacterial infections. In: P LJ G, Kleiman NS, and Page CP, editors. Platelets in Thrombotic and Non- thrombotic Disorders - Pathophysiology, Pharmacology and Therapeutics: an Update. Cham (Switzerland): Springer; 2017. p. 1071–1084.
[75] Kraemer BF, Campbell RA, Schwertz H, et al. Bacteria differentially induce degradation of Bcl-xL, a survival protein, by human platelets. Blood. 2012;120(25):5014–5020.
[76] Rondina MT, Garraud O. Emerging evidence for platelets as immune and inflammatory effector cells. Front Immunol. 2014;5:653.
[77] Paul M, Hemshekhar M, Kemparaju K, et al. Aggregation is impaired in starved platelets due to enhanced autophagy and cellular energy depletion. Platelets. 2019;30(4):487–497.
[78] Balasubramaniam S, Riley LG, Vasudevan A, et al. EPG5-Related Vici Syndrome: a Primary Defect of Autophagic Regulation with an Emerging Phenotype Overlapping with Mitochondrial Disorders. JIMD Rep. 2018;42:19–29.
[79] Byrne S, Jansen L, U-King-Im J-M, et al. EPG5-related Vici syndrome: a paradigm of neurodevelopmental disorders with defective autophagy. Brain. 2016;139(3):765–781.
[80] Hedberg-Oldfors C, Darin N, Oldfors A. Muscle pathology in Vici syndrome–A case study with a novel mutation in EPG5 and a summary of the literature. Neuromuscul Disord. 2017;27(8):771–776.

[81] Hori I, Otomo T, Nakashima M, et al. Defects in autophagosome-lysosome fusion underlie Vici syndrome, a neurodevelopmental disorder with multisystem involvement. Sci Rep. 2017;7(1):3552.
[82] Lee J-H, Yu WH, Kumar A, et al. Lysosomal proteolysis and autophagy require presenilin 1 and are disrupted by Alzheimer-related PS1 mutations. Cell. 2010;141(7):1146–1158.
[83] Tong J, Yan X, Yu L. The late stage of autophagy: cellular events and molecular regulation. Protein Cell. 2010;1(10):907–915.
[84] Noda T, Fujita N, Yoshimori T. The late stages of autophagy: how does the end begin? Cell Death Differ. 2009;16(7):984–990.
[85] Laursen MA, Larsen JB, Larsen KM, et al. Platelet function in patients with septic shock. Thromb Res. 2020;185:33–42.
[86] Tunjungputri RN, van de Heijden W, Urbanus RT, et al. Higher platelet reactivity and platelet-monocyte complex formation in Gram-positive sepsis compared to Gram-negative sepsis. Platelets. 2017;28(6):595–601.
[87] New J, Thomas SM. Autophagy-dependent secretion: mechanism, factors secreted, and disease implications. Autophagy. 2019;15(10):1682–1693.
[88] Banerjee M, Huang Y, Ouseph MM, et al. Autophagy in Platelets. Methods Mol Biol. 2019;1880:511–528.
[89] Button RW, Roberts SL, Willis TL, et al. Accumulation of autophagosomes confers cytotoxicity. J Biol Chem. 2017;292(33):13599–13614.
[90] Macintosh RL, Ryan KM. Autophagy in tumour cell death. Semin Cancer Biol. 2013;23(5):344–351.
[91] Claushuis TAM, van Vught LA, Scicluna BP, et al. Thrombocytopenia is associated with a dysregulated host response in critically ill sepsis patients. Blood. 2016;127(24):3062–3072.
[92] Assinger A, Schrottmaier WC, Salzmann M, et al. Platelets in Sepsis: an Update on Experimental Models and Clinical Data. Front Immunol. 2019;10:1687.
[93] Kuchitsu Y, Fukuda M. Revisiting Rab7 Functions in Mammalian Autophagy: rab7 Knockout Studies. Cells. 2018;7(11):215.
[94] Gutierrez MG, Munafo DB, Beron W, et al. Rab7 is required for the normal progression of the autophagic pathway in mammalian cells. J Cell Sci. 2004;117:2687–2697.
[95] Munford RS. Severe sepsis and septic shock: the role of gram-negative bacteremia. Annu Rev Pathol. 2006;1:467–496.
[96] D'Atri LP, Rodriguez CS, Miguel CP, et al. Activation of toll-like receptors 2 and 4 on CD34(+) cells increases human megakaryo/thrombopoiesis induced by thrombopoietin. J Thromb Haemost. 2019;17:2196–2210.
[97] Akira S, Uematsu S, Takeuchi O. Pathogen recognition and innate immunity. Cell. 2006;124:783–801.
[98] Kawasaki T, Kawai T. Toll-like receptor signaling pathways. Front Immunol. 2014;5:461.
[99] Xu Y, Jagannath C, Liu XD, et al. Toll-like receptor 4 is a sensor for autophagy associated with innate immunity. Immunity. 2007;27:135–144.
[100] Dionisi Vici C, Sabetta G, Gambarara M, et al. Agenesis of the corpus callosum, combined immunodeficiency, bilateral cataract, and hypopigmentation in two brothers. Am J Med Genet. 1988;29:1–8.
[101] Dellinger RP, Levy MM, Carlet JM, et al. Surviving Sepsis Campaign: international guidelines for management of severe sepsis and septic shock: 2008. Crit Care Med. 2008;36:296–327.
[102] Jones CA, London NR, Chen H, et al. Robo4 stabilizes the vascular network by inhibiting pathologic angiogenesis and endothelial hyperpermeability. Nat Med. 2008;14:448–453.
[103] Grubetamayer KS, Yserentant K, Herten DP. Photons in - numbers out: perspectives in quantitative fluorescence microscopy for in situ protein counting. Methods Appl Fluoresc. 2019;7:012003.
[104] Vangindertael J, Camacho R, Sempels W, et al. An introduction to optical super-resolution microscopy for the adventurous biologist. Methods Appl Fluoresc. 2018;6:022003.
[105] Wegel E, Gohler A, Lagerholm BC, et al. Imaging cellular structures in super-resolution with SIM, STED and Localisation Microscopy: a practical comparison. Sci Rep. 2016;6:27290.
[106] Mizushima N, Yoshimori T. How to interpret LC3 immunoblotting. Autophagy. 2007;3:542–545.
[107] Rubinsztein DC, Cuervo AM, Ravikumar B, et al. In search of an "autophagomometer". Autophagy. 2009;5:585–589.
[108] Kahr WH, Hinckley J, Li L, et al. Mutations in NBEAL2, encoding a BEACH protein, cause gray platelet syndrome. Nat Genet. 2011;43:738–740.
[109] Soderberg O, Gullberg M, Jarvius M, et al. Direct observation of individual endogenous protein complexes in situ by proximity ligation. Nat Methods. 2006;3:995–1000.
[110] Ono Y, Maejima Y, Saito M, et al. TAK-242, a specific inhibitor of Toll-like receptor 4 signalling, prevents endotoxemia-induced skeletal muscle wasting in mice. Sci Rep. 2020;10:694.
[111] Takashima K, Matsunaga N, Yoshimatsu M, et al. Analysis of binding site for the novel small-molecule TLR4 signal transduction inhibitor TAK-242 and its therapeutic effect on mouse sepsis model. Br J Pharmacol. 2009;157:1250–1262.